

# COUPLER KICKS IN THE THIRD HARMONIC MODULE FOR THE XFEL\*

E. Gjonaj<sup>#</sup>, W. Ackermann, T. Lau, T. Weiland, TU Darmstadt, TEMF,  
Schlossgartenstr. 8, 64289 Darmstadt, Germany  
M. Dohlus, DESY, Notkestr. 85, 22607 Hamburg, Germany

## Abstract

The rf and wakefield transverse kicks resulting from the asymmetry of input and HOM couplers in the third harmonic module for the XFEL are investigated. The fundamental mode is computed using eigenvalue analysis. The short range wakefields in a string of cavities are simulated with the PBCI code. Using the simulation data, the transverse kick factors associated with the presence of cavity couplers are evaluated.

## INTRODUCTION

The third harmonic system for the European XFEL at DESY will be largely based on the design developed at FNAL [1]. A single 3.9GHz cavity contains 9 cells, an input coupler, and two Higher Order Mode (HOM) couplers (see also Fig. 1a). The presence of these couplers breaks the rotational symmetry of the structure. It generates two types of unwanted beam-cavity interactions. First, a beam travelling on-axis will receive a transverse (rf-) kick because of the asymmetry of the fundamental mode. Second, broadband wakefields are excited at the couplers which give rise to an additional, self induced (wake-) transverse kick on the beam. Both interactions lead to emittance growth, and thus to loss of beam quality. The situation is very similar to the standard 1.3GHz TESLA cavities for the ILC and XFEL linacs. The coupler kicks in that case were thoroughly investigated in a series of recent papers [2,3]; the overall effect on the beam was estimated to be low. Similar evidence for the 3.9GHz system is so far missing. Preliminary calculations show that rf kick factors per cavity may be as much as 10 times larger than in TESLA cavities [4]. A more rigorous numerical analysis is, however, necessary in order to verify these results. In this paper, the fundamental mode fields in the 3.9GHz cavity as well as the wakefields in a sting of up to 4 cavities are numerically computed. The resulting field data are used to evaluate the kick factors associated with the presence of cavity couplers.

## FUNDAMENTAL MODE FIELDS

The discretization of the eigenvalue problem for cavity fields leads to a set of algebraic equations of the form:

$$\mathbf{C}^T \mathbf{C} \mathbf{e} - \omega^2 \mathbf{M} \mathbf{e} = 0. \quad (1)$$

In (1),  $\mathbf{C}$  and  $\mathbf{M}$  are discrete *curl* and *mass* operators, respectively;  $\mathbf{e}$  denotes the discrete electric (or magnetic) field unknowns and  $\omega$  is the mode frequency. In the

following, equation (1) is solved numerically for a full size third harmonic cavity including couplers in order to determine the 3D field distribution of the fundamental mode. Figure 1b shows the resulting electric mode pattern on the horizontal plane. The field distribution in the coupler regions is shown in Fig. 1c-d. Note the electric field increase occurring within the notch gaps and along the inner cavity parts of the two HOM couplers.

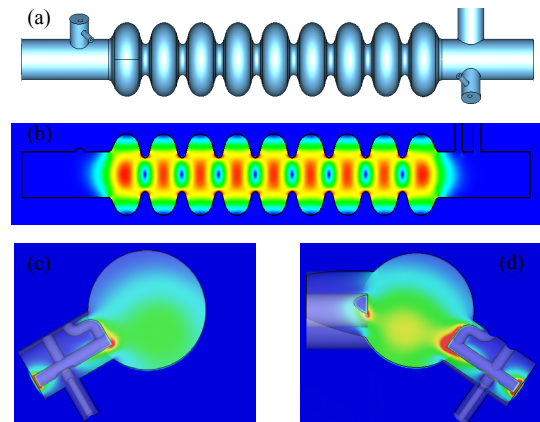


Figure 1: (a) Geometry of a 3.9GHz cavity. (b) Electric field strength of the fundamental mode on the horizontal plane, (c) in the upstream and (d) downstream couplers.

The electric field components on-axis normalized to a peak input power of 1W are shown in Fig. 2 and 3. The red curves depict the solution when the two HOM couplers are omitted. The contribution of the input coupler on the x-component of the electric field on-axis is approximately half as large as that of a HOM coupler (see Fig. 2). Furthermore, note that transverse fields penetrate from the two coupler regions through the neighbouring 2-3 cells from each side of the cavity. The full size cavity computation of the fundamental mode as performed here is, thus, justified.

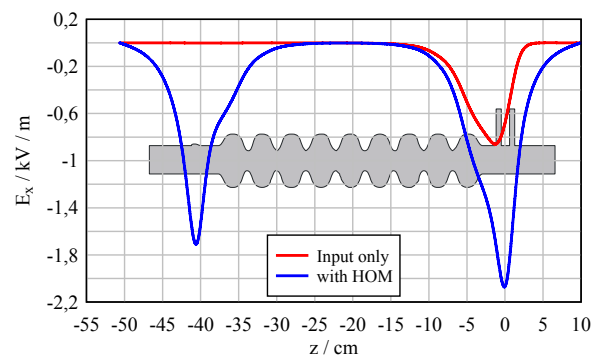


Figure 2: Electric field on the cavity axis (x-component).

\*Work supported by DESY

<sup>#</sup>gjonaj@temf.tu-darmstadt.de

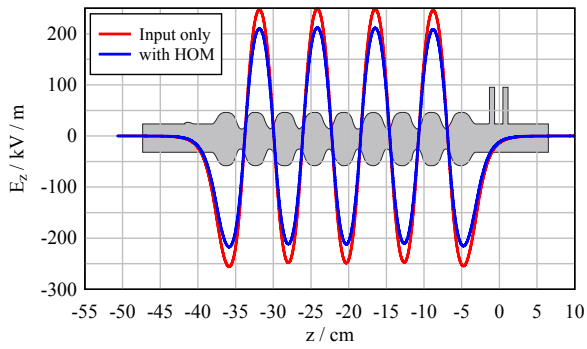


Figure 3: Electric field on the cavity axis (z-component).

It can be seen in Fig. 3 that adding HOM couplers to the cavity influences its external Q. The simulations yield an external Q factor of  $0.89 \cdot 10^6$  for the cavity with HOM couplers as compared to  $1.25 \cdot 10^6$  when omitting them. The transverse rf kicks can be computed directly from the numerical field data. Assuming off-crest acceleration, the figures shown in Table 1 are obtained. Note the partial compensation of the imaginary part of the kick factor in the x-direction which is due to the opposite orientations of upstream and downstream couplers. The resulting factors are still up to one order of magnitude larger than those obtained in [3] for the TESLA cavities. This result is in acceptable agreement with the estimations given in [4] using HFSS and MWS simulations.

Table 1: Transverse rf kicks in the 3.9GHz cavity

	$10^6 \times V_x / V_z$	$10^6 \times V_y / V_z$
Input only	$-182.0 + 50.05 i$	$0.271 + 0.066 i$
Downstream	$-378.0 - 96.19 i$	$65.71 + 199.9 i$
Upstream	$-140.8 + 262.5 i$	$-57.88 + 168.0 i$
Total	$-519.6 + 166.3 i$	$7.839 + 367.9 i$

### NUMERICAL ISSUES

The numerical solution of (1) for the fundamental mode is by far the most challenging task in this investigation. As seen in Fig. 3 and 4, the interesting transversal component is  $\sim 1000$  times smaller than the accelerating field. Thus, the numerical accuracy must be higher than  $10^{-5}$  in order to properly resolve this component. This fact was previously observed in [2,5] in rf kick computations concerning the 1.3GHz TESLA cavities. It appears that, such a numerical resolution cannot be easily achieved by merely refining the mesh. Below, two solution approaches on tetrahedral and Cartesian meshes are described.

#### Solution on Tetrahedral Meshes

The eigenvalue problem (1) is formulated in terms of the classical finite element method using linear and second order vectorial basis functions. In particular, applying the latter basis functions in combination with the Jacobi-Davidson algorithm for non-dissipative problems is a well established approach for electromagnetic modal analysis. As shown in Fig. 4 (blue line), however, the numerical solution for the y-component on a generic

tetrahedral mesh exhibits large parasitic oscillations. The high frequency noise is less critical and may be associated with the discrete representation of fields on the mesh. The long wave oscillations are related with numerical errors of the much larger longitudinal z-component. These errors disappear very slowly when the mesh is refined. A better way is to apply a truly symmetric mesh. The smooth (red) curve in Fig.4 is obtained by enforcing mirror symmetry on (most of) the tetrahedral mesh with respect to the transversal directions. This approach results in exact cancellation of the longitudinal field errors on-axis.

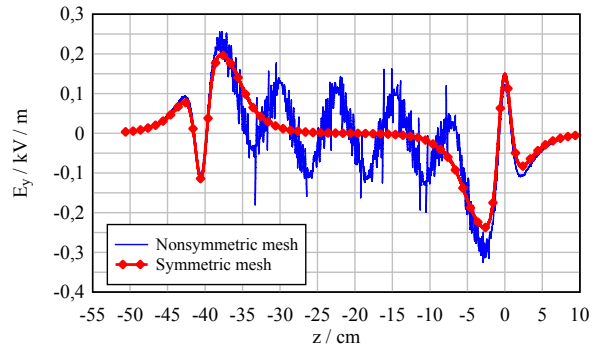


Figure 4: Electric field on the cavity axis (y-component).

#### Solution on Cartesian Meshes

Generating symmetric tetrahedral meshes “by hand” for complicated geometries may be difficult. Alternatively, the finite integration technique (FIT) on Cartesian meshes can be applied. The cancellation of longitudinal field errors on-axis here is easily imposed. However, the due accuracy can be only attained when a boundary conformal technique with partially filled cells (PFC) is applied. The drawback is the large condition number of the resulting algebraic equations. Given the numerical size of the problem (with more than  $2 \cdot 10^8$  mesh points) most of the iterative solvers used for the solution of (1) fail to reach convergence. To remedy, a hybridization of the (well conditioned) staircase and PFC discretizations is proposed. A geometry parameter  $\theta$  is introduced which mixes the crude geometrical approximation of staircase with the fine representation of PFC. Starting with staircase, the hybrid approximation is a few times iteratively improved until convergence is reached (see Fig. 5).

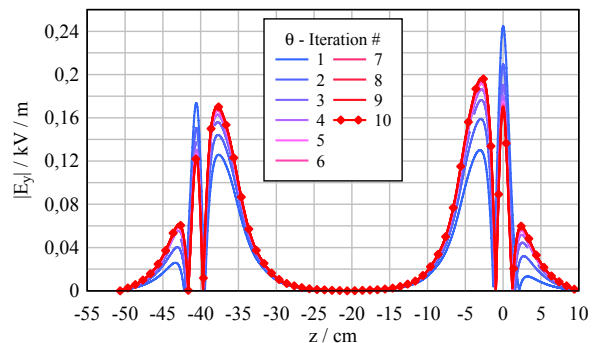


Figure 5: Convergence of the y-component of the electric field on-axis with respect to the geometry parameter  $\theta$ .

## WAKEFIELDS

The wakefields induced in the third harmonic system are computed with the PBCI code. In the simulations, a Gaussian bunch of rms length 2mm and rms radius 0.35mm is used. Smooth numerical convergence is achieved for a discretization with 8-10 grid points / bunch length within the moving simulation window of PBCI. A single cavity configuration as well as a full third harmonic module with 4 cavities (see Fig. 7) is considered.

Figure 6 shows the transverse wake potentials resulting from the simulation of a single 3.9GHz cavity with the outgoing beam pipe extending to infinity. The reader is referred to [2,3] for an equivalent investigation of the wakefields in the standard TESLA cavities. The wake amplitudes found here are 2-3 times larger than those presented in [2] for a single 1.3GHz cavity. Note that, there a shorter bunch ( $\sigma_z = 1\text{mm}$ ) was considered. The figure of comparison, however, remains valid since (as checked in separate calculations) the wake amplitudes depend weakly on the bunch length. The resulting transverse kick factors are almost equal;  $k_x = -31\text{V/nC}$  and  $k_y = -29.9\text{V/nC}$ , respectively.

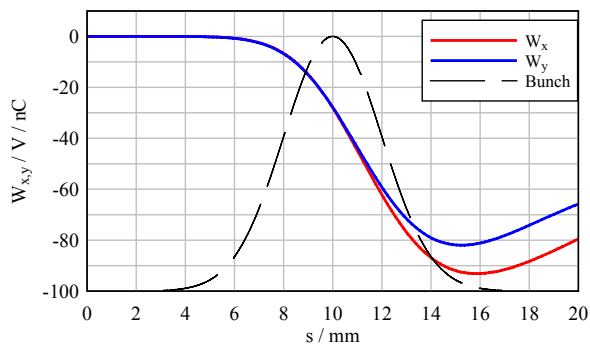


Figure 6: Transverse wake potentials for a single cavity.

In the following, cavity strings with up to 4 cavities are considered. A distance of  $3\lambda/2$  between neighbouring cavities is assumed, where  $\lambda \approx 7.7\text{cm}$  is the wave length of the fundamental mode. The periodicity of the problem suggests that on-axis cancellation of the total wake (as well as rf) kicks can be achieved by alternating the orientations of the couplers and/or cavities. A possible configuration where every second cavity is rotated around the z-axis is shown in Fig 7b (cf. [4]). A simpler module with identical cavities is depicted in Fig. 7a.

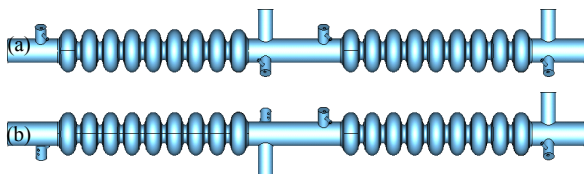


Figure 7: (a) Simple string configuration with identical cavities. (b) String configuration with rotated cavities.

Figure 8 and 9 show the wake potentials for the string configurations (a) and (b), respectively. The single lines depict the potentials measured in the intermediate beam pipe, at the exit of each cavity. As seen in Fig. 8, the

wake potentials for configuration (a) increase linearly with propagation length. Single cavity wake contributions simply add-up as the bunch passes a cavity. Then, it should be expected that for configuration (b) the wake contributions of neighbouring cavities exactly cancel. This is clearly observed in Fig. 9. The only contribution left is that of the last coupler, no matter how long the string is. This behaviour is due to the comparatively long bunches appearing in the 3.9GHz section. The low frequency wakes are quickly damped in the intermediate pipes, so that each cavity contributes individually to the total wake potential. Thus, wakefield kicks can be well controlled by modifying the cavity orientations. The kick factors found for configuration (a) are  $k_x = -122.5\text{V/nC}$  and  $k_y = -117.9\text{V/nC}$ , respectively. In the wakefield compensated case with rotated cavities  $k_x = 0.75\text{V/nC}$  and  $k_y = 0.9\text{V/nC}$  is found.

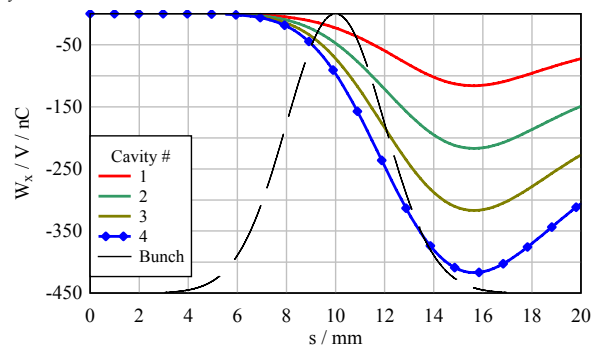


Figure 8: Transverse wake potential ( $W_x$ ) at the exit of each cavity for the string configuration in Fig. 7a.

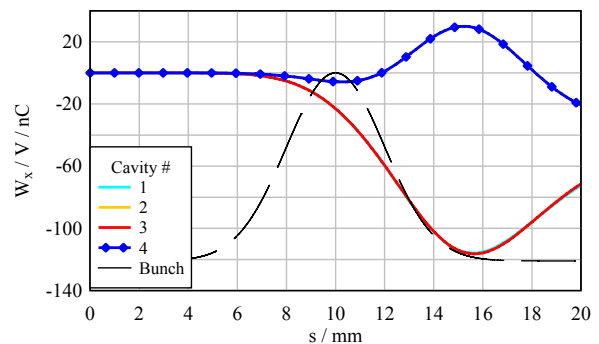


Figure 9: Transverse wake potential ( $W_x$ ) at the exit of each cavity for the string configuration in Fig. 7b.

## REFERENCES

- [1] E. Harms et al., "Status of 3.9GHz superconducting cavity technology at Fermilab", LINAC08, THP028.
- [2] K. Bane et al., "Wakefield and rf kicks due to coupler asymmetry in TESLA-type accelerating cavities", EPAC08, TUPP019.
- [3] M. Dohlus et al., "Coupler kicks for very short bunches and its compensation", EPAC08, MOPP013.
- [4] M. Dohlus, "Rf kick of 3<sup>rd</sup> harmonic cavities", [http://www.desy.de/xfel-beam/data/talks/talks/dohlus\\_-\\_kick\\_of\\_3rd\\_harm\\_20080317.pdf](http://www.desy.de/xfel-beam/data/talks/talks/dohlus_-_kick_of_3rd_harm_20080317.pdf)
- [5] N. Solyak, "Rf kick in the ILC acceleration structure", EPAC08, MOPP042.